

Supporting Information for

The Curious Case of Mesityl Azide and Its Reactivity with bpyNiEt₂

Brooke M. Otten, Travis M. Figg, Thomas R. Cundari*

Full Citation for Reference 27

Gaussian 09, Revision A.01, Frisch, M. J.; Trucks, G. W.; Schlegel, H. B.; Scuseria, G. E.; Robb, M. A.; Cheeseman, J. R.; Scalmani, G.; Barone, V.; Mennucci, B.; Petersson, G. A.; Nakatsuji, H.; Caricato, M.; Li, X.; Hratchian, H. P.; Izmaylov, A. F.; Bloino, J.; Zheng, G.; Sonnenberg, J. L.; Hada, M.; Ehara, M.; Toyota, K.; Fukuda, R.; Hasegawa, J.; Ishida, M.; Nakajima, T.; Honda, Y.; Kitao, O.; Nakai, H.; Vreven, T.; Montgomery, J. A., Jr.; Peralta, J. E.; Ogliaro, F.; Bearpark, M.; Heyd, J. J.; Brothers, E.; Kudin, K. N.; Staroverov, V. N.; Kobayashi, R.; Normand, J.; Raghavachari, K.; Rendell, A.; Burant, J. C.; Iyengar, S. S.; Tomasi, J.; Cossi, M.; Rega, N.; Millam, N. J.; Klene, M.; Knox, J. E.; Cross, J. B.; Bakken, V.; Adamo, C.; Jaramillo, J.; Gomperts, R.; Stratmann, R. E.; Yazyev, O.; Austin, A. J.; Cammi, R.; Pomelli, C.; Ochterski, J. W.; Martin, R. L.; Morokuma, K.; Zakrzewski, V. G.; Voth, G. A.; Salvador, P.; Dannenberg, J. J.; Dapprich, S.; Daniels, A. D.; Farkas, Ö.; Foresman, J. B.; Ortiz, J. V.; Ciosowski, J.; Fox, D. J. Gaussian, Inc., Wallingford CT, 2009.

Table S-1. Calculated free energies (a.u.) along with number of computed imaginary frequencies (nimag) are given for all computed species.

File Name	G (a.u.)	nimag	Comment
H_dot	-0.5109	0	H atom
NN_31+	-109.5399	0	N ₂
ethylene	-78.5621	0	ethylene
ethyl_rad	-79.1262	0	Et radical
MeN3_s	-204.0732	0	MeN ₃
butane	-158.3561	0	butane
etn3	-243.3644	0	ethyl azide
ph	-231.5080	0	phenyl radical
ArN	-286.2018	0	PhN singlet
ArN_t	-286.2528	0	PhN triplet
otol_ArN_t	-325.5466	0	T-oTolN
ptol_ArN_t	-325.5478	0	T-pTolN
PhN3_H_s	-395.7728	0	PhN ₃ singlet
PhN3_H_t	-395.7224	0	PhN ₃ triplet
mxyl_ArN_t	-364.8400	0	T-mXyN
amide	-365.4636	0	N(Et)Ph
ad_o_tolyl	-435.0651	0	oTolN ₃
MECP_otol_feq	-435.0103	0	MECP for oTolN ₃ = nitrene + N ₂
ad_p_tolyl	-435.0671	0	pTolN ₃
MECP_ptol_feq	-435.0116	0	MECP for pTolN ₃ = nitrene + N ₂
Et_o_tolyl	-404.7471	0	oTolNEt radical
2Et_o_tolyl	-404.7563	0	oTolNEt radical, 2nd conf

Et_p_tolyl	-404.7580	0	pTolNEt radical
oTolEtNH	-405.3829	0	oTolEtNH
pTolEtNH	-405.3844	0	pTolEtNH
ad_m_xylyl	-474.3620	0	mXyN ₃
MECP_mxyl_freq	-474.3029		MECP for mXyN ₃ = nitrene + N ₂
mes_ArN_t	-404.1346	0	T-MesN
13triaz	-474.9110	0	1,3-triazenyl rad, Et(Ph)NNN
33triaz	-474.9140	0	3,3-triazenyl rad, Et(Ph)NNN
etnats	-474.9151	0	TS for NA of Et rad on PhN ₃
Et_m_xylyl	-444.0507	0	mXyNEt radical
2Et_m_xylyl	-444.0413	0	mXyNEt radical, 2nd conf
mXyEtNH	-444.6793	0	mXyEtNH
ad_mesityl	-513.6454	0	MesN ₃
MECP_mes_freq	-513.5908		MECP for MesN ₃ = nitrene + N ₂
Et_mesityl	-483.3325	0	MesNEt radical
MesEtNH	-483.9602	0	MesNeEtH
n2ph2	-572.6206	1	PhN=NPh
Nibpy	-2003.4283	0	bpyNi singlet
Nibpy_t	-2003.4562	0	bpyNi triplet
13triaz-mes	-592.7846	0	1,3-triazenyl rad, Et(Mes)NNN
33triaz-mes	-592.7882	0	3,3-triazenyl rad, Et(Mes)NNN
etnats-mes	-592.7878	1	NA TS for Et attack on MesN ₃
nin2	-2113.0107	0	bpyNi(η^2 -N ₂)
nin2-t	-2112.9999	0	triplet bpyNi(η^2 -N ₂)
an_o_tolyl	-651.2029	0	oTolN=NoTol
an_p_tolyl	-651.2084	0	pTolN=NpTol
NiEt_BETS_d	-2082.6077	1	β -H elim from d-bpyNiEt
bpyNiHeth	-2082.6147	0	bpyNi(H)(η^2 -C ₂ H ₄) doublet
Ni_Et_BDE_d	-2082.6370	0	bpyNiEt radical
Ni_Et_BDE_q	-2082.6130	0	bpyNiEt radical Q
bpyNiEt-ag	-2082.6276	0	agostic bpyNiEt, Cs
an_m_xylyl	-729.7928	0	mXyN=NmXy
Ni_etuu_s	-2161.7901	0	bpyNiEt ₂ up-up conf
Ni_Et_s	-2161.7920	0	bpyNiEt ₂ up-down conf
Ni_etuu_starter_t	-2161.7731	0	triplet bpyNiEt ₂ up-up conf
Ni_etud_starter_t	-2161.7626	0	triplet bpyNiEt ₂ up-down conf
re-mecp-1	-2161.7675		MECP for butane reductive elimination
re-mecp-3	-2161.7712		MECP for butane reductive elimination
NiEt_RETs_s	-2161.7355	1	RE TS for butane formation from bpyNiEt ₂
NiEt_RETs_t	-2161.7518	1	RE TS for butane formation from t-bpyNiEt ₂
an_mesityl	-808.3612	0	MesN=NMes
Ni_imide_s	-2289.7860	0	bpyNi=NPh
Ni_imide_t	-2289.7899	0	bpyNi=NPh triplet
nats	-2399.2203	1	TS for NA on PhN ₃ by bpyNi
nats-t	-2399.2438	1	TS for NA on PhN ₃ by bpyNi
bpyNi(N3Ph)-3mr	-2399.2744	0	bpyNi(N3Ph) - 3 memb ring
bpyNi(N3Ph)-3mr-t	-2399.2441	0	bpyNi(N3Mes) - 3 memb ring
bpyNi(N3Ph)-4mr	-2399.2652	0	bpyNi(N3Ph) - 4 memb ring
bpyNi(N3Ph)-4mr-t	-2399.2641	0	bpyNi(N3Ph) - 4 memb ring, opened up
bpyNiN3Ar-k1	-2399.2652	0	κ^1 -N-int collapsed back to 4mr

bpyNi(N3Ph)-lin	-2399.2589	0	bpyNi(N3Ph) - κ^1 -coord
bpyNi(N3Ph)-lin-t	-2399.2543	0	more like a diazene
nin2nph	-2399.2860	0	bpyNi(NPh)(κ^1 -N ₂)
bpyNiamide	-2368.9905	0	bpyNi(N(Et)Ph)
bpyNiEtNPh	-2368.9333	0	bpyNi(Et)(NPh)
bpyNiEtNPh-b	-2368.9350	0	bpyNi(Et)(NPh) up-down conf
bpyNiamide-otol	-2408.2758	0	bpyNi(N(Et)oTol)
bpyNiamide-ptol	-2408.2821	0	bpyNi(N(Et)pTol)
naetts-d1	-2478.3945	1	NA TS for bpyNiEt/PhN ₃
naetts-d2	-2478.3819	1	NA TS for bpyNiEt/PhN ₃
bpyNiamide-mxy	-2447.5760	0	bpyNi(N(Et)mXy)
NiEt2_adduct_s	-2448.0471	0	bpyNi(Et) ₂ (NPh)
NiEt2_adduct_t	-2448.0503	0	bpyNi(Et) ₂ (NPh) triplet
NiEt_Ninsert_s	-2448.0340	1	singlet TS for PhN ₃ /bpyNi(Et) ₂
NiEt_Ninsert_t	-2448.0057	1	triplet TS for PhN ₃ /bpyNi(Et) ₂
prod	-2448.1300	0	bpyNi(Et)(N(Et)Ph)
nats-mes-t	-2517.1154	1	TS for NA on MesN ₃ by bpyNi
3mr-mes	-2517.1432	0	bpyNi(N ₃ Mes) - 3 memb ring
bpyNiamide-mes	-2486.8537	0	bpyNi(N(Mes)Et)
NiEt_Ninsert_ptol_t	-2487.2993	1	Et migration TS for bpyNi(NpTol)(Et)2
Ni_etdd_NIPH_s	-2487.4212	0	p-tol product
Ni_Ninsert_ptol_s	-2487.3267	1	TS for imide insertion p-tol
Ni_Ninsert_ptol_t	-2487.2993	1	TS for imide insertion p-tol
Ni_Ninsert_otol_s	-2487.3196	1	TS for imide insertion o-tol
Ni_Ninsert_otol_s	-2487.4070	0	oTol amide prod
Ni_Ninsert_ptol_s	-2487.4234	0	pTol amide prod
NiEt_Ninsert_mxyll_t	-2526.5909	1	Et migration TS for bpyNi(NmXy)(Et) ₂
Ni_Ninsert_mxyll_s	-2526.6192	1	TS for insertion of mXyN
nin2ph2	-2576.1214	0	S-bpyNi(PhN=NPh)
Ni_Ninsert_mxyll_s	-2526.7164	0	mXy amide prod
oTol_K_bpy	-2596.8207	0	bpyNi(Et)2(oTolN3)
oTol_KNb_bpy	-2596.8208	0	bpyNi(Et)2(oTolN3)
pTol_K_bpy	-2596.8142	0	bpyNi(Et)2(pTolN3)
pTol_etuKNb_bpy	-2596.8229	0	bpyNi(Et)2(pTolN3)
pTol_KNb_bpy	-2596.8274	0	bpyNi(Et)2(pTolN3)
Ni_etdd_N3Ph_Nucl_TS_s	-2596.7968	1	TS for pTolN3/bpyNi(Et)2, singlet, down-down conf
Ni_etud_N3Ph_Nucl_TS_s	-2596.7978	1	TS for pTolN3/bpyNi(Et)2, singlet, up-down conf
Ni_etuu_N3Ph_Nucl_TS_s	-2596.8019	1	TS for pTolN3/bpyNi(Et)2, singlet, up-up conf
Ni_etuu_N3Ph_Nucl_TS_t	-2596.8043	1	TS for pTolN3/bpyNi(Et)2, triplet, up-up conf
Ni_etud_N3Ph_Nucl_TS_t	-2596.8076	1	TS for pTolN3/bpyNi(Et)2, triplet, up-down conf
Ni_etdd_N3Ph_Nucl_TS_t	-2596.8095	1	TS for pTolN3/bpyNi(Et)2, triplet, down-down conf
o_Tol_etud_a_s	-2596.7921	1	TS for oTolN3/bpyNi(Et)2, singlet, up-down conf
o_Tol_etdd_a_s	-2596.7924	1	TS for oTolN3/bpyNi(Et)2, singlet, down-down conf
o_Tol_etud_a_t	-2596.8003	1	TS for oTolN3/bpyNi(Et)2, triplet, up-down conf
o_Tol_etuu_a_s	-2596.7989	1	TS for oTolN3/bpyNi(Et)2, singlet, up-up conf
o_Tol_etuu_a_t	-2596.8025	1	TS for oTolN3/bpyNi(Et)2, triplet,down-down conf
o_Tol_etdd_a_t	-2596.8076	1	TS for oTolN3/bpyNi(Et)2, triplet, down-down conf
Ni_Ninsert_mes_s	-2565.9758	0	Mes amide prod
13	-2685.5309	1	TS for 1,3-dipolar addition of PhN ₃ to bpyNi=NPh
13t	-2685.5363	1	TS for 1,3-dipolar addition of PhN ₃ to bpyNi=NPh
mX_KNb_bpy	-2636.1194	0	bpyNi(Et) ₂ (mXyN ₃)

Ni_etdd_N3mX_TS_s	-2636.0892	1	TS for mXyN ₃ /bpyNi(Et) ₂
Ni_etuu_mX_TS_s	-2636.0940	1	TS for mXyN ₃ /bpyNi(Et) ₂
Ni_etuu_mX_TS_t	-2636.1024	1	TS for mXyN ₃ /bpyNi(Et) ₂
Ni_etdd_N3Ph_Nucl_TS_t	-2636.1052	1	TS for mXyN ₃ /bpyNi(Et) ₂
tet	-2685.5974	1	S-bpyNi(1,4-Ph ₂ -N ₄)
tet-t	-2685.5990	1	T-bpyNi(1,4-Ph ₂ -N ₄)
mes_etuKNb_bpy	-2675.4033	0	bpyNi(Et) ₂ (MesN ₃)
mes_KNb_bpy	-2675.4054	0	bpyNi(Et) ₂ (MesN ₃)
namests	-2675.3892	1	NA TS for MesN ₃ on bpyNiEt ₂

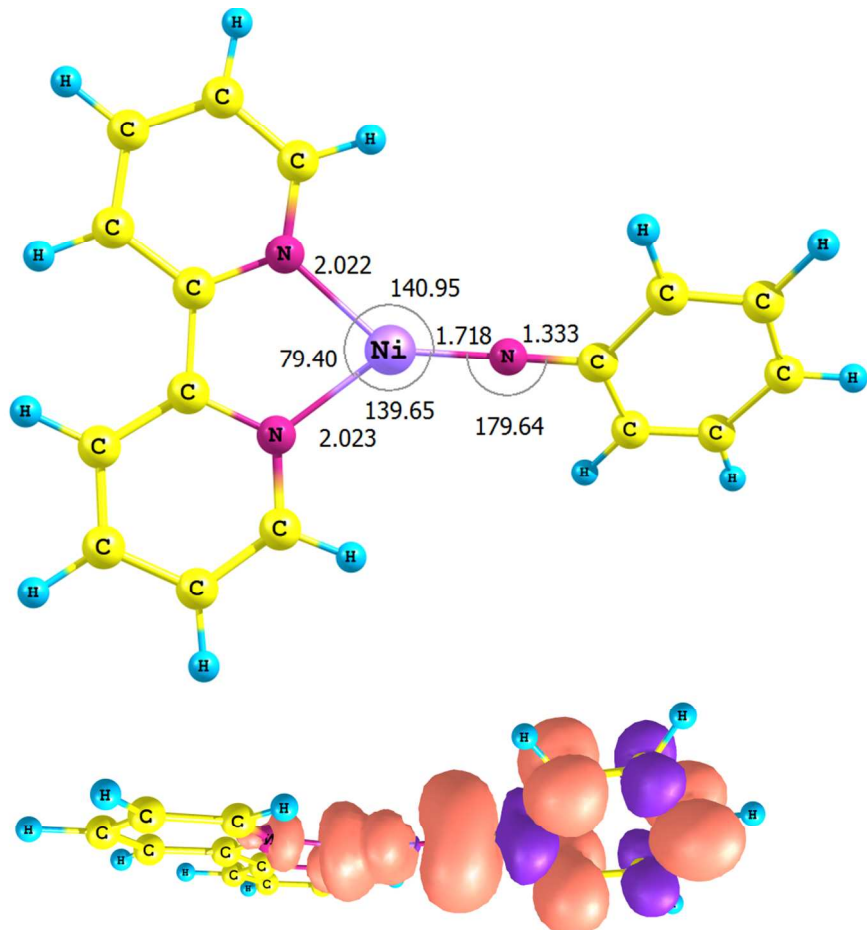


Figure S-1. DFT-optimized structure of $^{3}\text{bpyNi}=\text{NPh}$ (top) and computed spin density (bottom).

Metal-free Reactions

a. $\text{ArN}_3 \rightarrow \text{N}_2 + {}^3\text{ArN}$

Computations were employed to assess whether the differences observed by Lin^{Error! Bookmark not defined.} might be due to intrinsic reactivity differences in the aryl azides. To this end, several reactions were probed; the first of these was loss of N_2 and formation of a triplet aryl nitrene. For the parent PhN_3 , the calculated singlet-triplet gap (ΔG_{ST}) was 32 kcal/mol in favor of the triplet. While this value may not be qualitatively reliable due to the multiconfigurational nature of singlet aryl nitrenes, focus was given to triplet nitrenes to the large (ΔG_{ST}).

i. Thermodynamics

The most intriguing thermodynamic result for dinitrogen loss was for mesityl azide, **Table S-1**, which was ~5 kcal/mol more exergonic than the same reaction for other aryl azides. In conjunction with the geometry differences discussed above, this implied that destabilization of the ground state of the mesityl azide by the flanking 2- and 6-methyl groups was *ca.* 5 kcal/mol. *Hence, one may propose from the above calculated “organic” thermodynamics that mesityl azide would be the most intrinsically reactive of the reagents investigated experimentally*, making the observed differences in reactivity that much more mysterious, and suggesting metal-based reactions as the root cause.

ΔH (kcal/mol)	ΔG (kcal/mol)	Reaction
-2.0	-13.4	$\text{oTolN}_3 \rightarrow \text{N}_2 + {}^3\text{oTolN}$
-2.0	-12.9	$\text{pTolN}_3 \rightarrow \text{N}_2 + {}^3\text{pTolN}$
-1.6	-11.2	$\text{mXyN}_3 \rightarrow \text{N}_2 + {}^3\text{mXyN}$
-6.8	-18.2	$\text{MesN}_3 \rightarrow \text{N}_2 + {}^3\text{MesN}$

Table S-1. B3LYP/6-31+G(d) energetics for loss of N_2 from ArN_3 .

ΔH (kcal/mol)	ΔG (kcal/mol)	Reaction
33.4	34.4	$\text{oTolN}_3 \rightarrow \text{oTol_MECP}$
32.4	34.8	$\text{pTolN}_3 \rightarrow \text{pTol_MECP}$
32.4	37.1	$\text{mXyN}_3 \rightarrow \text{mXy_MECP}$
31.6	34.3	$\text{MesN}_3 \rightarrow \text{Mes_MECP}$

Table S-2. Calculated minimum energy crossing points for ${}^1\text{ArN}_3 \rightarrow {}^1\text{N}_2 + {}^3\text{ArN}$.

ii. Minimum Energy Crossing Points

In light of the exergonicity of the fission of aryl azides into dinitrogen and triplet aryl nitrene, **Table 1**, the barrier to spin crossing was assessed between the singlet azide reactant (ArN_3) and the triplet nitrene product (${}^3\text{ArN} + \text{N}_2$). For example, the triplet state of PhN_3 was calculated to be more than 31 kcal/mol uphill (ΔG) from its singlet ground state. The protocol of Harvey^{Error! Bookmark not defined.} was employed to calculate the minimum energy crossing points (MECPs) in the reaction $\text{ArN}_3 \rightarrow \text{N}_2 + {}^3\text{ArN}$. As can be seen in **Table 2**, the calculated singlet-triplet crossing points were relatively insensitive to substitution on the aryl ring, ranging from $\Delta G_{\text{MECP}} = 34$ (oTolN_3) – 37 (mXyN_3 and MesN_3) kcal/mol. Note that the enthalpy and free energy corrections of the singlet MECP “stationary point” were used to convert the MECP electronic energies to approximate enthalpies and free energies.

Representative geometries of the calculated MECP for expulsion of N_2 from MesN_3 and ${}^3\text{MesN}$ are shown in **Figure S-2**. The NN bond length for the nascent N_2 is 1.184 Å versus 1.105 Å for free N_2 at the same B3LYP/6-31+G(d) level of theory. As another point of comparison, NN = 1.262 Å in azomesitylene (*vide infra*) and 1.143 Å in MesN_3 . The NN bond being broken is 1.394 Å in the MECP versus 1.235 Å in MesN_3 . Finally, the bond length calculated between the *ipso* carbon and nitrogen of the incipient nitrene is 1.358 Å in the MECP and 1.433 Å in the ground state of MesN_3 ; the same bond length in ${}^3\text{MesN}$ is calculated to be 1.320 Å.

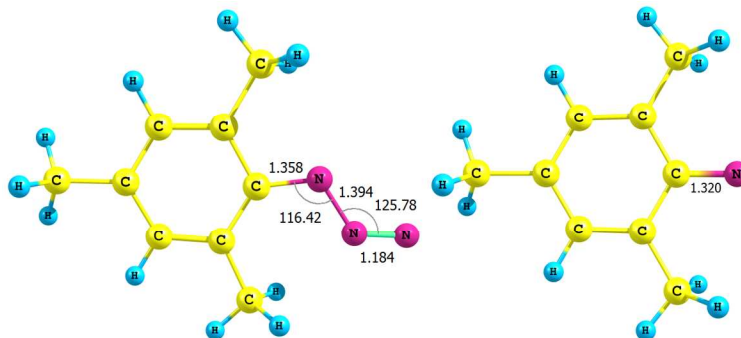


Figure S-2. DFT-optimized minimum energy crossing point (MECP) – singlet and triplet surfaces – for expulsion of N_2 from MesN_3 (left) and ground state of $^3\text{MesN}$.

The calculated MECP free energies relative to their corresponding aryl azide ground states implied that despite the thermodynamic driving force for expulsion of N_2 from aryl azides, *a sizeable barrier of > 34 kcal/mol must be surmounted to produce free triplet aryl nitrene that might then react with organonickel species.*

ΔH (kcal/mol) ΔG (kcal/mol) Reaction

-86.3	-95.6	$2 \text{oTolN}_3 \rightarrow 2 \text{N}_2 + \text{oTolN=NpTol}$
-89.1	-96.9	$2 \text{pTolN}_3 \rightarrow 2 \text{N}_2 + \text{pTolN=NpTol}$
-87.8	-93.2	$2 \text{mXyN}_3 \rightarrow 2 \text{N}_2 + \text{mXyN=NmXy}$
-86.1	-94.2	$2 \text{MesN}_3 \rightarrow 2 \text{N}_2 + \text{MesN=NMes}$

Table S-3. DFT calculated energetics of azo formation.

b. $2 \text{ArN}_3 \rightarrow \text{ArN=NAr} + 2 \text{N}_2$

Lin reported, among other organic products, the formation of azo compounds, ArN=NAr , Error! Bookmark not defined. which is usually good evidence of nitrene intermediates, either free or complexed to nickel. To assess the former, the thermodynamics of azo formation were compared for the aryl azides studied experimentally. There was little spread in the calculated thermodynamics among pTolN₃, oTolN₃, mXyN₃ and MesN₃, **Table S-3**. As expected for a reaction producing two equivalents of dinitrogen, the coupling of two aryl azides to make an azo compound was highly exergonic, $\Delta G = -95 \pm 2$ kcal/mol.

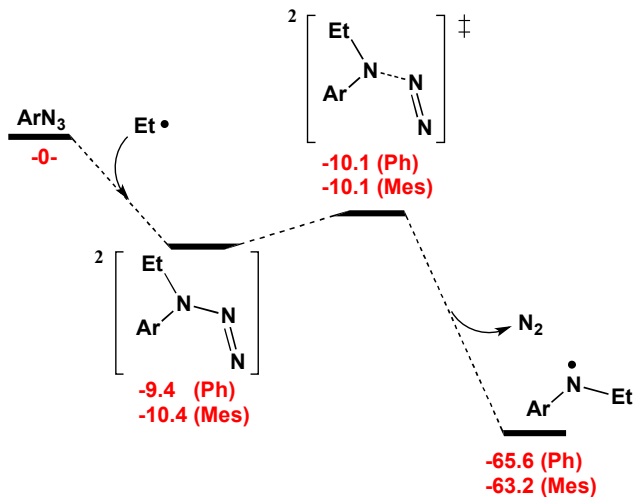
ΔH (kcal/mol)	ΔG (kcal/mol)	Reaction
-68.3	-65.8	$\text{oTolN}_3 + \text{Et}^\bullet \rightarrow \text{oTolN}^\bullet(\text{Et}) + \text{N}_2$
-68.7	-65.8	$\text{pTolN}_3 + \text{Et}^\bullet \rightarrow \text{pTolN}^\bullet(\text{Et}) + \text{N}_2$
-68.8	-64.3	$\text{mXyN}_3 + \text{Et}^\bullet \rightarrow \text{mXyN}^\bullet(\text{Et}) + \text{N}_2$
-66.0	-63.2	$\text{MesN}_3 + \text{Et}^\bullet \rightarrow \text{MesN}^\bullet(\text{Et}) + \text{N}_2$

Table S-4. DFT calculated energetics for addition of ethyl radical to aryl azide to form dinitrogen and amide radical.

c. $\text{ArN}_3 + \text{Et}^\bullet \rightarrow \text{ArN}^\bullet(\text{Et}) + \text{N}_2$

As a final “metal-free” reaction to be modeled, addition of ethyl radical (produced via homolytic cleavage of a Ni—Et bond of bpyNiEt₂) to aryl azide to make an aminyl radical was calculated. *As with the coupling reaction just discussed, there was a modest spread of values as a function of aryl group, $\Delta G = -65 \pm 1$ kcal/mol, for a very exergonic reaction, Table S-4.* Calculation of the transition state for loss of N_2 via a 3,3-ethyl,aryl-triazenyl radical ($\text{Ar}(\text{Et})\text{NNN}^\bullet$) showed nearly identical (*i.e.*, barrierless) free energies for Ar = Mes and Ph, **Scheme S-1**, further supporting the supposition that the intrinsic reactivity of aryl azides was quite similar, and that organic reactions would presumably not differentiate MesN₃ from the other aryl azides. By extension, one may surmise that the origin of these differences entails the

reactivity of ArN_3 with a nickel complex. The computed N—H bond enthalpies for $(\text{Ar}(\text{Et})\text{N})\text{—H}$ are $\sim 81 - 82$ kcal/mol, suggestive of a very weak bond and a stable aminyl radical. So, it is likely that aminyl radicals could have an appreciable lifetime in the THF solution used experimentally and persist long enough to react with other radicals in solution such as bpyNiEt^\bullet .



Scheme S-1. Pathway for reaction of ethyl radical with aryl (phenyl, Ph; mesityl, Mes) azides to make an aminyl radical ($\text{ArN}^\bullet(\text{Et})$). Free energies (kcal/mol, in red) were calculated at 298.15 K and 1 atm.